edge-linked PC pairs can be seen in Fig. 5(*c*). The latter type of PC pairs, however, is the building unit in the $Mo_{17}O_{47}$ structure (Kihlborg, 1960).

We are grateful to Professor Lars Kihlborg for valuable comments on the manuscript and Mrs Gunvor Winlöf for skilful photographic work. This study was supported by the Swedish Natural Science Research Council.

References

De Pape, R., Gauthier, G. & Hagenmuller, P. (1968). *C. R. Acad. Sci.* **266**, 803-805.
Deschanvres, A., Frey, M., Raveau, B. & Thomazeau, J. (1968). *Bull. Soc. Chim. Fr.* **9**, 3519-3523.
Hörlin, T., Marinder, B.-O. & Nygren, M. (1982). *Rev. Chim. Miner.* **19**, 231-238.
Kihlborg, L. (1960). *Acta Chem. Scand.* **14**, 1612-1622.
Kihlborg, L. & Klug, A. (1973). *Chem. Scr.* **3**, 207-211.
Li, D. Y., Lundberg, M., Werner, P.-E. & Westdahl, M. (1984). *Acta Chem. Scand. Ser. A*, **38**, 813-817.
Lundberg, M. (1971). *Chem. Commun. Univ. Stockholm*, No. XII.
Lundberg, M. & Sundberg, M. (1986). *J. Solid State Chem.* **63**, 216-230.
Lundberg, M., Sundberg, M. & Magnéli, A. (1982). *J. Solid State Chem.* **44**, 32-40.
Magnéli, A. (1949). *Ark. Kemi*, **1**, 223-230.
Obayashi, H. & Anderson, J. S. (1976). *J. Solid State Chem.* **17**, 79-89.
O'Keefe, M., Buseck, P. R. & Iijima, S. (1978). *Nature (London)*, **274**, 322-324.
Sahle, W. & Sundberg, M. (1980). *Chem. Scr.* **16**, 163-168.
Sleight, A. (1966). *Acta Chem. Scand.* **20**, 1102-1112.
Smith, G. S. & Snyder, R. L. (1979). *J. Appl. Cryst.* **12**, 60-65.
Sundberg, M. & Lundberg, M. (1987). *Acta Cryst.* B**43**, 238-244.
Werner, P.-E. (1969). *Ark. Kemi*, **31**, 513-516.
Wolff, P. M. de (1968). *J. Appl. Cryst.* **1**, 108-113.

Acta Cryst. (1987). B**43**, 434-440

Anharmonic Thermal Vibrations in Wurtzite-Type AgI

By Akira Yoshiasa, Kichiro Koto, Fumikazu Kanamaru, Shuichi Emura and Hiroyuki Horiuchi*

The Institute of Scientific and Industrial Research, Osaka University, Mihoga-oka, Ibaraki, Osaka 567, *Japan*

(*Received* 16 *January* 1987; *accepted* 20 *May* 1987)

Abstract

The thermal behavior of atoms in β-AgI (wurtzite-type structure) was investigated by X-ray diffraction at 123, 297, 363 and 413 K. Determination of the accurate positional parameter and calculation of the probability density function (p.d.f.) were performed by applying a model of the cumulant-expansion up to fourth-order terms. The effective one-particle potentials (o.p.p.) of both Ag and I atoms along the Ag–I bond at each temperature were evaluated from the p.d.f. Several reflections which violate the extra conditions of the systematic absences were observed and explained by anharmonic thermal vibrations. The o.p.p. curves of both atoms disclosed softening of the potentials with increasing temperature. The p.d.f. maps also revealed that the thermal motions of both atoms are strongly anharmonic and that the degree of anisotropic thermal motion of the I atom becomes more prominent than that of the Ag atom at higher temperatures. The thermal motion of the I atom reveals a salient anharmonicity toward the structure transformation from β- to α-AgI. The magnitudes of the temperature factors are larger in mobile Ag atoms than in I atoms. The appreciable anisotropy of the thermal motions is not directly related to the macroscopic characteristics of ionic conduction. Crystal data: $M_r = 234{\cdot}772$, $P6_3mc$, $Z = 2$, Mo $K\alpha$, $\lambda = 0{\cdot}71069$ Å, $\mu = 18{\cdot}14$ mm^{-1}, $F(000) = 200$; at 123 K: $a = 4{\cdot}591$ (1), $c = 7{\cdot}511$ (4) Å, $V = 137{\cdot}1$ (1) Å^3, $D_x = 5{\cdot}708$ Mg m^{-3}, $R = 0{\cdot}023$ for 323 reflections; at 297 K: $a = 4{\cdot}592$ (1), $c = 7{\cdot}510$ (2) Å, $V = 137{\cdot}1$ (1) Å^3, $D_x = 5{\cdot}706$ Mg m^{-3}, $R = 0{\cdot}029$ for 170 reflections; at 363 K: $a = 4{\cdot}591$ (1), $c = 7{\cdot}508$ (2) Å, $V = 137{\cdot}0$ (1) Å^3, $D_x = 5{\cdot}710$ Mg m^{-3}, $R = 0{\cdot}020$ for 108 reflections; at 413 K: $a = 4{\cdot}590$ (1), $c = 7{\cdot}506$ (2) Å, $V = 137{\cdot}0$ (1) Å^3, $D_x = 5{\cdot}714$ Mg m^{-3}, $R = 0{\cdot}017$ for 90 reflections.

Introduction

The wurtzite-type silver iodide (β-AgI) shows a considerable ionic conductivity owing to diffusion of Ag ions even at room temperature. It exhibits a negative thermal expansion, and undergoes a first-order phase transition at 420 K to the superionic conducting phase, α-AgI, with higher density. The cleavage and gliding perpendicular to the *c* axis occur because of the anisotropy of interatomic force.

* Present address: Mineralogical Institute, Faculty of Science, Tokyo University, Hongo, Tokyo 113, Japan.

0108-7681/87/050434-07$01.50

Table 1. *Cell dimensions and atomic parameters in the harmonic and anharmonic models*

Bond distances and angles were calculated based on the results of the anharmonic model. Ag* indicates the apical atom of the trigonal pyramid.

	123 K		297 K		363 K		413 K	
Cell dimensions	*a*	*c*	*a*	*c*	*a*	*c*	*a*	*c*
(Å)	4·591 (1)	7·511 (4)	4·592 (1)	7·510 (2)	4·591 (1)	7·508 (2)	4·590 (1)	7·506 (2)
Harmonic model	$R = 0{\cdot}025$	$wR = 0{\cdot}031$	0·046	0·051	0·038	0·045	0·044	0·049
	I	Ag	I	Ag	I	Ag	I	Ag
z	0·0	0·6257 (1)	0·0	0·6274 (5)	0·0	0·6278 (8)	0·0	0·6289 (10)
$\beta_{11}\times10^4$	235 (2)	356 (3)	629 (7)	975 (14)	793 (12)	1253 (23)	936 (17)	1487 (35)
$\beta_{33}\times10^4$	71 (1)	108 (1)	163 (2)	271 (5)	214 (4)	346 (8)	251 (5)	413 (10)
Anharmonic model	$R = 0{\cdot}023$	$wR = 0{\cdot}028$	0·029	0·030	0·020	0·020	0·017	0·018
	I	Ag	I	Ag	I	Ag	I	Ag
z	0·0	0·6247 (3)	0·0	0·6274 (8)	0·0	0·6267 (10)	0·0	0·6273 (10)
$\beta_{11}\times10^4$	243 (5)	365 (8)	668 (17)	1059 (26)	851 (21)	1372 (32)	981 (25)	1638 (38)
$\beta_{33}\times10^4$	76 (2)	110 (3)	161 (5)	279 (6)	221 (6)	367 (8)	250 (7)	442 (9)
$\gamma_{111}\times10^6$	−30 (27)	351 (65)	62 (68)	2199 (203)	207 (94)	3293 (293)	209 (127)	4717 (391)
$\gamma_{333}\times10^6$	52 (10)	−52	134 (38)	−134	310 (60)	−310	429 (74)	−429
$\gamma_{113}\times10^6$	−23 (15)	23	−380 (73)	380	−540 (116)	540	−813 (144)	813
$\delta_{1111}\times10^6$	8 (7)	11 (17)	137 (38)	394 (94)	218 (57)	668 (150)	260 (83)	1119 (216)
$\delta_{3333}\times10^6$	2 (1)	2 (2)	−4 (4)	31 (10)	0 (6)	53 (16)	−8 (8)	94 (20)
$\delta_{1113}\times10^6$	−11 (14)	−14 (15)	−3 (32)	−15 (36)	−98 (80)	−24 (78)	−94 (43)	−4 (64)
$\delta_{1133}\times10^6$	2 (1)	1 (2)	1 (4)	14 (12)	12 (6)	22 (17)	15 (9)	40 (24)
Bond distances (Å)								
Ag–I	2·811 (1)		2·819 (2)		2·816 (3)		2·817 (3)	
Ag*–I	2·819 (3)		2·798 (6)		2·803 (8)		2·797 (8)	
Ag–Ag	4·591 (1)		4·592 (1)		4·591 (1)		4·590 (1)	
Ag*–Ag	4·597 (2)		4·597 (1)		4·595 (1)		4·594 (1)	
Bond angles (°)								
Ag–I–Ag	109·48 (4)		109·1 (1)		109·2 (2)		109·1 (2)	
Ag–I–Ag*	109·47 (5)		109·8 (1)		109·7 (1)		109·8 (2)	

Mair & Barnea (1975) presented a detailed theoretical study of anharmonic thermal vibrations in wurtzite-type structures. Several X-ray studies on the anharmonic thermal vibration of wurtzite-type compounds have been reported (*e.g.* Whiteley, Moss & Barnea, 1978; Stevenson, Milanko & Barnea, 1984; Kihara & Donnay, 1985). Cava, Reidinger & Wuensch (1977) refined the structure of α-AgI using neutron diffraction and showed that the complex Ag-atom distribution is completely accounted for by higher-order thermal tensors. Piltz & Barnea (1987) have studied anharmonicity of β-AgI using X-ray diffraction at room temperature and revealed the presence of considerable cubic anharmonic effects.

The dispersion relation of the normal modes of lattice vibration in β-AgI was determined based on the coherent neutron inelastic scattering experiments of Bührer & Brüesch (1975) and Bührer, Nicklow & Brüesch (1978). They reported that the characteristics of phonon spectra showed some strong anharmonic effects, and analyzed a peculiar dispersion relation by a valence-shell model. Beyeler, Brüesch, Hibma & Bührer (1978) calculated the diffuse scattering pattern of β-AgI with parameters of the valence-shell model. They concluded that β-AgI exhibits a low-frequency phonon-induced diffuse scattering but no additional diffuse scattering due to static disorder. The large temperature factors of both atoms, therefore, should not be attributed to the statistical distribution.

In this work we studied the behavior of anharmonic thermal vibrations in β-AgI as a function of temperature by the X-ray diffraction method, and the effect of chemical-bond character on the anharmonicity. We applied the cumulant-expansion formalism proposed by Johnson (1969, 1970) in order to determine the accurate positional parameters and the probability density function (p.d.f.) at 123, 297, 363 and 413 K. The mechanism of ionic conduction of β-AgI is discussed based on the thermal vibration of atoms. The crystal chemistry of the wurtzite-type compounds is also discussed based on the results of the structure of β-AgI.

Experimental

Specimen

β-AgI single crystals were grown by the method reported by Cochrane (1967). As the crystals are easily cleaved normal to the *c* axis, a single crystal used for X-ray work was carefully ground to a sphere by hand using emery paper under a microscope. The spherical crystal with a diameter of 0·20 mm was examined by means of precession photography before intensity measurements.

Temperature dependence of cell dimensions

Cell dimensions at various temperatures between 115 and 413 K were determined by the least-squares method using the 2θ values of fifteen reflections within the range $20° < 2\theta < 50°$ measured on a Rigaku AFC5FOS four-circle diffractometer (Table 1, Fig. 1). Mo $K\alpha$ radiation ($\lambda = 0{\cdot}71069$ Å) monochromatized by pyrolytic graphite was obtained from a rotating-anode X-ray generator (60 kV, 200 mA). The same set of fifteen reflections was used in all the measurements. Temperature fluctuations were within ±2 K.

Intensity measurements

Accurate intensity measurements of 1359, 1338, 1125 and 491 Bragg reflections at 123, 297, 363 and 413 K, respectively, were made. Intensities of reflections within one quadrant were measured adopting the θ–2θ scan mode, scan width of $1{\cdot}8° + 0{\cdot}8° \tan\theta$ and scan speed of $5° \text{ min}^{-1}$ in 2θ. Reflections were measured within $(\sin\theta)/\lambda < 1{\cdot}15$ Å^{-1}. Lorentz and polarization factors were applied and absorption correction for spherical shape was made; $\mu r = 1{\cdot}81$, min., max. transmission coefficients = 0·092, 0·164. The significant intensities with $|F_o| > 3\sigma(|F_o|)$ were observed within 1·04, 0·82 and 0·78 Å^{-1} of $(\sin\theta)/\lambda$ at 297, 363 and 413 K, respectively (84, 133, 155, 64 reflections unobserved at 123, 297, 363, 413 K). Independent reflections were obtained by averaging the equivalent reflections and are 323 at 123 K, 170 at 297 K, 108 at 363 K and 90 at 413 K. The amplitude variations of standard reflections throughout the measurements were within ±1·7% at 413 K. The deviations from the averaged values of $|F_o|$ of equivalent reflections were within about 2·5%. The corrections

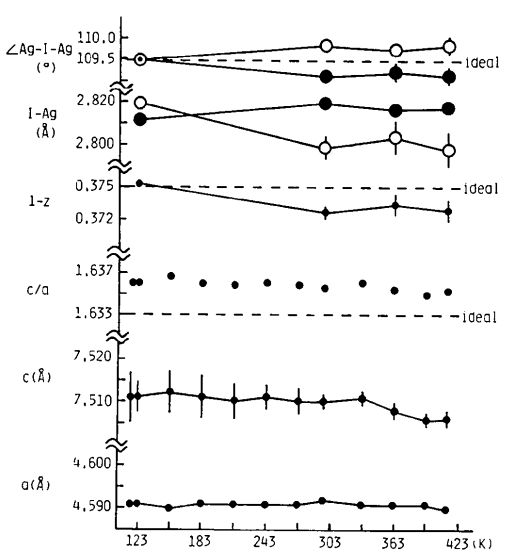

Fig. 1. The temperature variation of the cell dimensions (a, c), axial ratio (c/a), coordinate of Ag atom ($1-z$), bond distances (I-Ag) and angles (∠Ag-I-Ag) in β-AgI: ○, apical (*i.e.* including the apex of the trigonal pyramid; ●, basal.

for thermal diffuse scattering (TDS) were made by adopting a model of first-order scattering due to a one-phonon process of the acoustic mode (Sakata & Harada, 1976). The program *TDS2* (Stevens, 1974) was used for the evaluation of the TDS correction factor. The elastic constants for each temperature were taken from Fjeldly & Hanson (1974).

Refinement of the structure

Refinements were carried out using the program *RFINE4* (Finger & Prince, 1975). Cumulant expansion up to fourth-order terms was applied to the temperature factors. The temperature factor $T(\mathbf{h})$ is expressed as

$$T(\mathbf{h}) = \exp[(i^2/2!)\sum\sum\beta_{jk}h_jh_k + (i^3/3!)\sum\sum\sum\gamma_{jkl}h_jh_kh_l + (i^4/4!)\sum\sum\sum\sum\delta_{jklm}h_jh_kh_lh_m]$$

(Johnson, 1969, 1970), where β_{jk}, γ_{jkl} and δ_{jklm} are the coefficients in the second-, third- and fourth-order cumulant terms, respectively. In order to calculate $T(\mathbf{h})$ with a harmonic model for β-AgI, four independent coefficients β_{jk} and the positional parameter z for Ag are necessary. The anharmonic model required fourteen additional independent coefficients γ_{jkl} and δ_{jklm} (seven for each atom); γ_{111} $(=-\gamma_{222}=2\gamma_{112}=-2\gamma_{122})$, γ_{333}, γ_{113} $(=\gamma_{223}=2\gamma_{123})$, δ_{1111} $(=\delta_{2222}=2\delta_{1112}=2\delta_{1222}=2\delta_{1122})$, δ_{3333}, δ_{1113} $(=-\delta_{2223}=2\delta_{1123}=-2\delta_{1223})$ and δ_{1133} $(=\delta_{2233}=2\delta_{1233})$ (referred to *International Tables for X-ray Crystallography*, 1974). In addition, a scale factor and an isotropic extinction factor are included in the least-squares refinements ($g = 0{\cdot}67\times10^{-8}$, $0{\cdot}77\times10^{-8}$, $0{\cdot}34\times10^{-7}$, $0{\cdot}31\times10^{-7}$ at 123, 297, 363, 413 K). Simultaneous refinement of the four independent terms, γ_{333}(I), γ_{333}(Ag), γ_{113}(I), γ_{113}(Ag) was unsuccessful because of the strong correlations between γ_{333}(I) and γ_{333}(Ag), and between γ_{113}(I) and γ_{113}(Ag). Then constraints of $\gamma_{333}(\text{I}) = -\gamma_{333}(\text{Ag})$ and $\gamma_{113}(\text{I}) = -\gamma_{113}(\text{Ag})$ were adopted, which are the same as used by Kihara & Donnay (1985). Atomic scattering factors for neutral atoms and correction terms for anomalous dispersion were taken from *International Tables for X-ray Crystallography* (1974).

The alternatives of indexing hkl and $\bar{h}\bar{k}\bar{l}$ are possible because of the non-centrosymmetric structure. The correct choice was decided based on the comparison of the final R factors $[=\sum(||F_o|-|F_c||)/\sum|F_o|]$ for both cases. The difference in the R factors between the alternatives was 0·2% for the 297 K data. The results of the refinements and the experimental conditions are given in Table 1.* The

* Lists of structure factors and a table of experimental data have been deposited with the British Library Document Supply Centre as Supplementary Publication No. SUP 44012 (7 pp.). Copies may be obtained through The Executive Secretary, International Union of Crystallography, 5 Abbey Square, Chester CH1 2HU, England.

refinements based on the anharmonic model remarkably reduced the R factor compared with those based on the harmonic model. Consequently, it is concluded that the anharmonic model is essential to the β-AgI structure. Maxima in positive and negative electron densities in the difference-Fourier maps for the data at 413 K were 0·28 and $-0{\cdot}43$ e Å^{-3}, respectively, after the refinements with the anharmonic model. Bond distances and angles are plotted *versus* temperature in Fig. 1. The p.d.f. maps computed using the *PDFED* program (Kihara, Matsumoto & Imamura, 1986) are presented in Fig. 2.

The effective one-particle potential (o.p.p.) of an isolated atom, $V(\mathbf{r})$, is derived from the p.d.f. by the following equation (Willis, 1969; Bachmann & Schulz, 1984):

$$V(\mathbf{r}) = V_0 - kT \ln [\text{p.d.f.}(\mathbf{r})],$$

where k is the Boltzmann constant, T is the absolute temperature, and V_0 is an arbitrary numerical factor. The o.p.p. curves of both atoms along the basal Ag–I bond at individual temperatures are plotted in Fig. 3.

Results and discussion

Anharmonic thermal vibrations and forbidden reflections

The wurtzite-type structure belongs to space group $P6_3mc$. Because both Ag and I atoms are located in Wyckoff positions 2(b), the site symmetry of which is $3m$, the systematic absence of reflections has extra conditions provided that atomic thermal vibrations are harmonic. That is, reflections of hkl with $h-k=3n$ are absent if l is odd in addition to the normal systematic absence. However, these reflections were observed to have intensities owing to the strong anharmonicity of thermal vibrations in β-AgI (Fig. 4). Agreement of the observed structure amplitudes among the equivalent reflections was reasonable. Agreement of the observed and calculated structure amplitudes for these reflections is good in the anharmonic model mentioned above (Table 2).

Whiteley, Moss & Barnea (1978) reported that the paired reflections 70l and 53l with the same l value (non-symmetry-related reflections with the same Bragg angle) of the wurtzite-type structure can have different amplitudes in the anharmonic model, whereas they must have the same amplitudes in the harmonic one. In β-AgI significant differences in amplitudes between 70l and 53l were observed (Table 3). This characteristic is the same as in other wurtzite-type structures (Stevenson & Barnea, 1984; Kihara & Donnay, 1985).

The p.d.f. maps (Fig. 2) revealed that the motions of both atoms are strongly anharmonic even at lower temperature. The o.p.p. is given with the assumption that an atom independently vibrates within the range of the average potential caused by the interaction

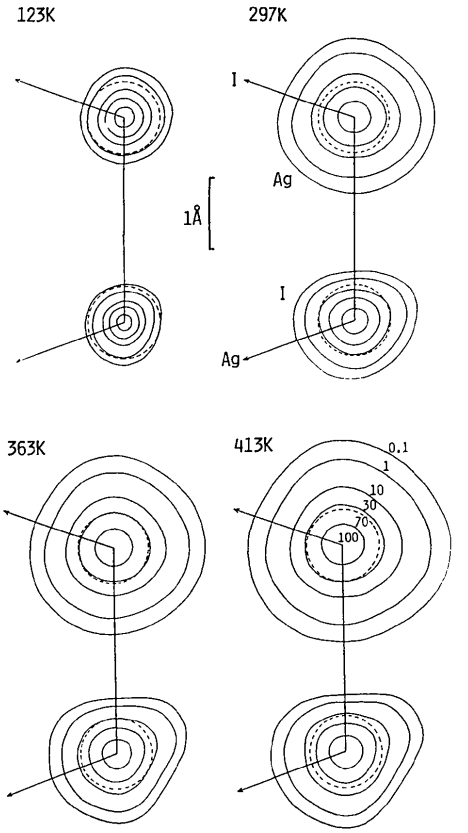

Fig. 2. The probability density function on (11$\bar{2}$0). The contours are scaled to 100 units at the centers. The broken lines are 0·5 Å from the centers.

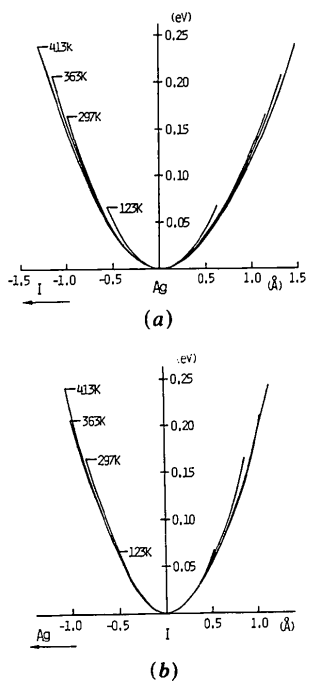

Fig. 3. Effective one-particle potentials of (a) Ag and (b) I atoms in β-AgI along the basal Ag–I bond, showing the potential curves at 123, 297, 363 and 413 K.

with all the other atoms in the crystal. The o.p.p. curves of both atoms (Fig. 3) revealed the softening of the potentials with increasing temperature, and should also justify the validity of the thermal tensor coefficients (Table 1) obtained independently from each data set.

Structure changes and temperature dependence of anharmonic thermal vibrations

Fig. 1 shows structure changes of β-AgI as a function of temperature up to the vicinity of the phase-transition point. In the ideal wurtzite-type structure based on hexagonal closest packing, the axial ratio (c/a), a variable coordinate $1-z$ and the bond angle are $(8/3)^{1/2}$, 0·375 and 109·47°, respectively. With increasing temperature, $1-z$ and the bond angles of β-AgI diverge from the ideal values, whereas the axial ratio which is slightly larger than the ideal value at lower temperature approaches the ideal one. The manner of the decrease in the axial ratio with temperature is similar to other wurtzite-type compounds (*e.g.* Mair & Barnea, 1975; Kihara & Donnay, 1985). The axial ratio is closely related to the elongation or compression of AgI_4 or Ag_4I tetrahedra along the c axis. The c axis becomes short when the temperature is raised. With increasing temperature, the apical Ag–I distance (parallel to the c axis) becomes shorter whilst the other three basal Ag–I distances become slightly larger. The three apical bond angles become larger whilst the other three basal bond angles become smaller. The shortening of the apical bond distance makes the three apical bond angles larger as illustrated in Fig. 5.

These structural changes *versus* temperature can be explained by the anharmonic thermal vibration, especially for the I atom. The anharmonic thermal vibrations of both atoms in β-AgI are demonstrated in the p.d.f. maps (Fig. 2). The anisotropy of thermal motion of the I atom becomes predominant over that of the Ag atom at higher temperature. If we compare the magnitudes of vibrations of I atoms along four antibonding directions, the magnitude along the c axis is smaller than the other three equivalent magnitudes. This causes the centroid of thermal vibration of the I atom to deviate towards the apical Ag atom with increasing temperature, which is shown schematically in Fig. 5.

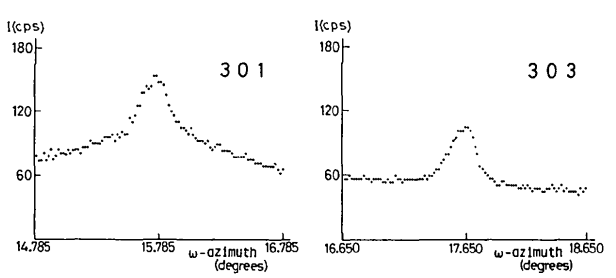

Fig. 4. Examples of the observed reflections violating the extra conditions of the systematic absences owing to the anharmonic thermal vibrations. The intensity distributions (counts s^{-1}) were obtained by θ–2θ scan mode.

Table 2. *Observed amplitudes of the reflections violating the extra conditions for systematic absences at room temperature*

These structure amplitudes can be explained by the anharmonic model.

h	k	l	$\lvert F_o\rvert$	$\lvert F_c\rvert$harmonic	$\lvert F_c\rvert$anharmonic
3	0	1	1·69 (9)	0·0	1·25
3	0	3	1·19 (11)	0·0	1·08
4	1	1	1·37 (9)	0·0	0·92

Table 3. *Structure amplitudes of reflections 70l and 53l at 123 K*

$\lvert F_c\rvert$'s were calculated with the anharmonic model.

h	k	l	$\lvert F_o\rvert$	$\lvert F_c\rvert$	$\sigma\lvert F_o\rvert$	h	k	l	$\lvert F_o\rvert$	$\lvert F_c\rvert$	$\sigma\lvert F_o\rvert$
7	0	0	7·61	7·88	0·15	5	3	0	8·47	8·55	0·13
7	0	1	6·75	6·89	0·15	5	3	1	6·82	7·11	0·15
7	0	2	5·95	5·93	0·16	5	3	2	6·26	6·21	0·16
7	0	3	12·67	12·41	0·12	5	3	3	12·18	12·15	0·12
7	0	5	10·44	10·82	0·13	5	3	5	10·61	10·56	0·12
7	0	6	4·01	4·55	0·17	5	3	6	4·39	4·39	0·15
7	0	7	4·90	4·98	0·14	5	3	7	5·34	5·07	0·16
7	0	8	4·48	4·43	0·16	5	3	8	4·93	4·57	0·14
7	0	11	4·34	4·49	0·14	5	3	11	4·30	4·37	0·14

Relation of anharmonicity to the phase transition and to the ionic conduction

The transition from β- to α-AgI of the body-centered lattice was discussed, based on the displacement of the I atom, by Burley (1967) and Bührer & Brüesch (1975). In Fig. 2, it is noted that, at higher temperature, the magnitudes of anharmonic thermal motion of the I atom are larger along the three antibonding directions. This makes the structure closer to the body-centered cubic arrangement of α-AgI. In β-AgI, Bührer & Brüesch (1975) observed a low-lying

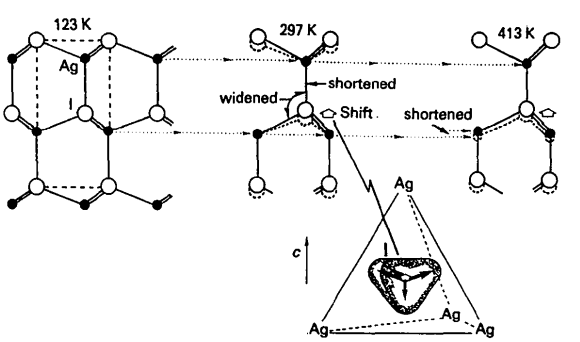

Fig. 5. Schematic representation of the structural changes in β-AgI with temperature. The position of the I atom shifts (white arrow) along the c axis owing to the anharmonic thermal vibrations. Thus, the c axis becomes shorter with increasing temperature.

Table 4. *Observed bond distances* (Å) *and angles* (°) *of various wurtzite-type compounds in order of decreasing Phillips ionicity* f_i

	f_i	$M-N^*$ † apical	$M-N$ basal	$\frac{M-N^*}{M-N}$	$\angle N^*-M-N$ apical	$\angle N-M-N$ basal	References	R factor
AgI (297 K)	0·77	2·798 (6)	2·819 (2)	0·993	109·8 (1)	109·1 (1)	This study	0·029
AgI (123 K)	0·77	2·819 (3)	2·811 (1)	1·003	109·5 (1)	109·5 (1)	This study	0·023
CdSe	0·70	2·6355 (5‡)	2·6299 (6)	1·002	109·31 (1)	109·63 (2)	Stevenson, Milanko & Barnea (1984)	0·007
CdS	0·69	2·5318 (7‡)	2·5263 (6)	1·002	109·05 (1)	109·89 (2)	Stevenson & Barnea (1984)	0·009
ZnO (473 K)	0·62	1·9892 (9)	1·9762 (6)	1·007	108·12 (3)	110·79 (3)	Kihara & Donnay (1985)	0·010
ZnO (293 K)	0·62	1·9884 (8)	1·9738 (4)	1·007	108·12 (2)	110·79 (2)	Kihara & Donnay (1985)	0·019
BeO	0·60	1·657 (7)	1·646 (2)	1·007	108·8 (2)	110·1 (2)	Sabine & Hogg (1969)	0·036
GaN	0·50	1·956 (4)	1·949 (1)	1·004	109·1 (1)	109·8 (1)	Schulz & Thiemann (1977)	0·041
AlN	0·45	1·903 (2)	1·889 (1)	1·007	108·11 (4)	110·80 (3)	Schulz & Thiemann (1977)	0·015

† N^* indicates the apical atom of trigonal pyramid.
‡ Calculated by assuming that the error in the cell dimensions was 0·001 Å.

optical mode which makes a large contribution to the thermal motion. They also demonstrated that this mode plays an important role in the displacement of the I atom on the phase transition. The displacements of the atoms in this mode mainly change the tetrahedral angles and slightly vary the Ag–I distances. The p.d.f. for the I atom along the antibonding direction of the basal Ag atoms will evidently satisfy the matter. Therefore, their interpretation of thermal motion applying a lattice-dynamical treatment agrees with our results obtained by the analysis based upon the intensities of the Bragg reflections.

The temperature factors of the mobile Ag atoms are larger than those of the I atoms (Table 1, Fig. 2). This accords well with the results of lattice-dynamical studies (Bührer & Brüesch, 1975; Bührer, Nicklow & Brüesch, 1978); *e.g.* their theoretical r.m.s. radial displacements of the Ag atoms at room temperature (0·292 Å) are comparable with our experimental ones [0·28 (1) Å: obtained from the equivalent isotropic temperature factor of the Ag atom at 297 K]. The ionic conductivity of β-AgI is due to Frenkel defects. The formation of Frenkel defects is closely related to the thermal motion of ions (Frenkel, 1926). Hence, the knowledge of the thermal motion should be of primary importance for understanding the ionic conduction. During the measurements of ionic conductivity on single crystals of β-AgI, it was found that the Ag-ion conductivity was essentially isotropic (Cava & Rietman, 1984). So it can be said that the appreciable anisotropy of the thermal motion in the hexagonal close-packed structure is not directly related to the macroscopic characteristics of ionic conduction in β-AgI.

Structural variations in wurtzite-type compounds

The wurtzite-type structure is closely related to the sphalerite-type structure. Both structures are classified into covalently bonded compounds. The notable difference in the environment around atoms in both structures is shown in Fig. 6. It is well known that wurtzite has a larger Madelung constant and is more ionic than sphalerite. Table 4 presents the bond distances, bond angles and ratios of the apical distance to the basal one for wurtzite-type compounds. As shown by the dotted lines in Fig. 6, the electrostatic interaction between an atom and its third neighbors in the wurtzite-type structure is greater than that in the sphalerite-type structure. Thus the apical distances for most of the compounds are longer than the basal ones except for β-AgI at room temperature. This is due to the electrostatic attraction and/or the difference in the contribution to hybridization between three directions and another symmetrically non-equivalent direction. In β-AgI (Fig. 1), the apical distance is longer than the basal ones at 123 K. However, it becomes shorter at higher temperature. Such a variation, as described above, results from the shortening of the apical bond distance owing to the anharmonic thermal vibrations.

With an increase in ionicity defined by Phillips (1970), the ratios $(M-N^*)/(M-N)$ decrease and accordingly the apical bond angles increase (Table 4). Since the electrostatic interaction should increase with the ionicity (f_i), the decrease in the ratios $(M-N^*)/(M-N)$ with the increase in ionicity is inconsistent. The thermal vibrations are generally dependent on the bonding force and thus the anharmonicity will cause the structural variations in the wurtzite-type

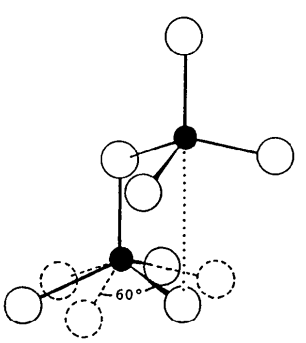

Fig. 6. Difference in the configurations of the third neighbor for wurtzite-type (solid line) and shalerite-type (broken line) structure.

compounds. Martin (1970) and Fjeldly & Hanson (1974) observed that the elastic properties of the covalently bonded sphalerite-type and wurtzite-type compounds show a systematic tendency towards lattice instability as the ionicity increases. Koto & Schulz (1979) have reported that the diffuse scattering increases in intensity with increasing ionicity. The tendency toward the lattice instability should result in the increase in anharmonicity.

We are grateful to Drs K. Kihara, Kanazawa University, and K. Tanaka, Tokyo Institute of Technology, for providing the computer programs. Thanks are also due to Mr T. Tanaka and Ms H. Yamamoto of this institute for helpful assistance. Discussions with and useful information from Dr S. Ohba, Keio University, and Professor M. Tokonami, University of Tokyo, are much appreciated. Intensity measurements were performed at the Materials Analyzing Center of this institute and all computations were carried out at the Crystallographic Research Center, Institute for Protein Research, Osaka University. Part of the expenses for this work were defrayed by a research grant from the Ministry of Education of the Japanese Government.

References

BACHMANN, R. & SCHULZ, H. (1984). *Acta Cryst.* A**40**, 668-675.
BEYELER, H. U., BRÜESCH, P., HIBMA, T. & BÜHRER, W. (1978). *Phys. Rev. B*, **18**, 4570-4575.
BÜHRER, W. & BRÜESCH, P. (1975). *Solid State Commun.* **16**, 155-158.
BÜHRER, W., NICKLOW, R. M. & BRÜESCH, P. (1978). *Phys. Rev. B*, **17**, 3362-3370.
BURLEY, G. (1967). *Acta Cryst.* **23**, 1-5.
CAVA, R. J., REIDINGER, F. & WUENSCH, B. J. (1977). *Solid State Commun.* **24**, 411-416.
CAVA, R. J. & RIETMAN, E. A. (1984). *Phys. Rev. B*, **30**, 6896-6902.
COCHRANE, G. (1967). *Br. J. Appl. Phys.* **18**, 687-688.
FINGER, L. W. & PRINCE, E. (1975). *Natl. Bur. Stand. (US) Tech. Note* No. 854.
FJELDLY, T. A. & HANSON, R. C. (1974). *Phys. Rev. B*, **10**, 3569-3577.
FRENKEL, J. (1926). *Z. Phys.* **35**, 652-669.
International Tables for X-ray Crystallography (1974). Vol. IV. Birmingham: Kynoch Press. (Present distributor D. Reidel, Dordrecht, The Netherlands.)
JOHNSON, C. K. (1969). *Acta Cryst.* A**25**, 187-194.
JOHNSON, C. K. (1970). *Thermal Neutron Diffraction*, edited by B. T. M. WILLIS, ch. 9. Oxford: Clarendon Press.
KIHARA, K. & DONNAY, G. (1985). *Can. Mineral.* **23**, 647-654.
KIHARA, K., MATSUMOTO, T. & IMAMURA, M. (1986). *Z. Kristallogr.* In the press.
KOTO, K. & SCHULZ, H. (1979). *Acta Cryst.* A**35**, 971-974.
MAIR, S. L. & BARNEA, Z. (1975). *Acta Cryst.* A**31**, 201-207.
MARTIN, R. M. (1970). *Phys. Rev. B*, **1**, 4005-4011.
PHILLIPS, J. C. (1970). *Rev. Mod. Phys.* **42**, 317-356.
PILTZ, R. O. & BARNEA, Z. (1987). *J. Appl. Cryst.* **20**, 3-7.
SABINE, T. M. & HOGG, S. (1969). *Acta Cryst.* B**25**, 2254-2256.
SAKATA, M. & HARADA, J. (1976). *Acta Cryst.* A**32**, 426-433.
SCHULZ, H. & THIEMANN, K. H. (1977). *Solid State Commun.* **23**, 815-819.
STEVENS, E. D. (1974). *Acta Cryst.* A**30**, 184-189.
STEVENSON, A. W. & BARNEA, Z. (1984). *Acta Cryst.* B**40**, 530-537.
STEVENSON, A. W., MILANKO, M. & BARNEA, Z. (1984). *Acta Cryst.* B**40**, 521-530.
WHITELEY, B., MOSS, G. & BARNEA, Z. (1978). *Acta Cryst.* A**34**, 130-136.
WILLIS, B. T. M. (1969). *Acta Cryst.* A**25**, 277-300.

Acta Cryst. (1987). B**43**, 440-448

Commensurate Ordering and Domains in the $Ba_{1\cdot2}Ti_{6\cdot8}Mg_{1\cdot2}O_{16}$ Hollandite

BY ERIC FANCHON, JEAN VICAT, JEAN-LOUIS HODEAU, PIERRE WOLFERS, DUC TRAN QUI AND PIERRE STROBEL

Laboratoire de Cristallographie, Centre National de la Recherche Scientifique, Laboratoire associé à l'USMG, 166X, 38042 Grenoble CEDEX, France

(*Received* 13 *February* 1987; *accepted* 26 *May* 1987)

Abstract

The $x = 1\cdot20$ compound of $Ba_xTi_{8-x}Mg_xO_{16}$ hollandite has been investigated by electron microscopy and X-ray diffraction. Hollandites are formed of a framework providing tunnels in which the cations (here Ba^{2+}) are located. The competition between Ba/framework interactions and Ba/Ba repulsion leads to superstructure reflections, which can be incommensurable in the tunnel direction. The electron images show the occurrence of microdomains, and it was necessary to take them into account in X-ray refinements. The experimental data and least-squares results are: $M_r = 775\cdot7$, monoclinic, $I2/m$, $a = 10\cdot227\ (3)$, $b = 14\cdot907\ (8)$, $c = 9\cdot964\ (6)$ Å, $\beta = 90\cdot77\ (4)°$, $V = 1519\ (2)$ Å^3, $Z = 5$, $D_x = 4\cdot24$ Mg m^{-3}, λ(Ag $K\alpha$) $= 0\cdot5608$ Å, $\mu = 4\cdot24$ mm^{-1}, $F(000) = 1796$, $T = 293$ K. Final $wR(F^2) = 0\cdot05$ for 1776 unique reflections. The structure inside ordered domains is characterized by the $m_0 = 5$ ···Ba(1)-[Ba(1)-□-Ba(2)-□-Ba(1)]··· sequence along the tunnels (□ = vacancy). The two adjacent Ba(1) cations are

0108-7681/87/050440-09$01.50